WEP Warwick Evans Publishing

Transactions on Engineering and Technology Research
ISSN: 2960-1797, eISSN: 2960-2246 | Volume 2
AMMEE 2024

STAR-RIS aided NOMA Networks: A Signal Enhancement Algorithm

Leyu Cao[1,a],Tianwei Hou[1,2,*],Anna Li[3,b], Xin Sun[1,c], Zhengyu Song[1,d], Jun Wang[1,e], Wei Chen[1,f]

[1]School of Electronic and Information Engineering, Beijing Jiaotong University, Beijing, China.

[2]Institute for Digital Communications, Friedrich-Alexander Universität Erlangen-Nürnberg (FAU), Erlangen, GER

[3]School of Computing and Communications, Lancaster University, Lancaster, UK

[a]21211234@bjtu.edu.cn

*twhou@bjtu.edu.cn

[b]anna.li@qmul.ac.uk

[c]xsun@bjtu.edu.cn

[d]songzy@bjtu.edu.cn

[e]wangjun1@bjtu.edu.cn

[f]weich@bjtu.edu.cn

Abstract. In order to overcome the reflecting-only issue of the conventional reconfigurable intelligent surface (RIS), simultaneous-transmitting-and-reflecting reconfigurable intelligent surface (STAR-RIS) stands as a potential solution for providing access services to the users located at the full space. By utilizing the omnidirectional properties of STAR-RIS, non-orthogonal multiple access (NOMA) users on both sides can be served simultaneously. By making the signal reflected by STAR-RIS coherent superposition with the direct signal, using the Riemannian optimization algorithm (ROA), the proposed signal enhancement algorithm can greatly enhance the signal power of NOMA users, reduce the outage probability, and improve the ergodic rate performance. According to the simulation results, the random phase STAR-RIS can improve the spectral efficiency of 3.6bit/s/Hz compared without STAR-RIS. After using the proposed ROA, the spectral efficiency can be extra increased by 1.8bit/s/Hz, which verifies the superiority of the proposed algorithm.

Keywords: simultaneous-transmitting-and-reflecting reconfigurable intelligent surface, non-orthogonal multiple access, signal enhancement algorithm, ergodic rate.

1. Introduction

In recent years, with the development of the sixth generation (6G) of mobile communication, higher requirements have been put forward for the capacity, coverage, energy efficiency and reliability of wireless communication networks [1]. Reconfigurable intelligent surface (RIS) as a potential technology of 6G, can significantly improve the spectral efficiency and energy efficiency of wireless communication. In wireless channels, signals undergo a series of complex processes such as reflection, refraction, scattering, diffraction, penetration, interference, etc. RIS can skillfully control the reflection phase of wireless signals, so that the wireless signal coherently enhances or coherently cancels at the user, improves the effective signal amplitude of the user, or inhibits the amplitude of interfering signals [2], [3]. At present, aiming at the disadvantage that the traditional RIS can only reflect wireless signals, a new simultaneous-transmitting-and-reflecting reconfigurable intelligent surface (STAR-RIS) has begun to receive attention. Through STAR-RIS, the transmission phase coefficient and reflection phase coefficient of the wireless signal are controlled at the same time, which can not only serve the users on the same side of RIS, but also serve the users on the rear side of STAR-RIS, and the coverage range can reach 360° [4], [5].

The traditional RIS only has the reflection metasurfaces layer, the control layer and the base layer, which can only control the amplitude and phase of the reflected signal, while the transmitted part of the radio wave has no controllability [6]. STAR-RIS has a reflective metasurfaces layer, a transmitted metasurfaces layer, a control layer and a base layer, which can independently control the amplitude and phase of the reflected signal and transmitted signal to realize the control of the amplitude and phase of the transmitted signal [7]. In terms of location deployment, STAR-RIS is also quite different from traditional RIS. The traditional RIS cannot control the transmitted signal, and it can be deployed on the wall surface of a tall building without considering the user's position behind the panel. On the contrary, STAR-RIS needs to be deployed on glass surfaces or roofs of tall buildings, allowing multiple users to be located on both sides of the STAR-RIS. It is worth mentioning that the reflection process and transmission process of STAR-RIS occur simultaneously, which not only has the simultaneity of signal transmission and reflection, but also has the simultaneity of signal processing. In addition, since the reflection user of STAR-RIS service is closer to the base station (BS), while the transmission user is farther away from the BS, the channel state information (CSI) of the reflection user is much stronger than that of the transmission user. It is ideal for non-orthogonal multiple access (NOMA) [8].

In 6G, NOMA shares time domain, frequency domain and code domain resources of multiple users with different CSI strengths. By using successive coding (SC) and successive interference cancellation (SIC) techniques, the ergodic rate of users is greatly improved [9], [10]. Furthermore, the research on improving RIS system with NOMA technology is still in its infancy. A signal enhancement based (SEB) algorithm was proposed in [11], in which the signal reflected by RIS is coherently superimposed at the user with the highest channel gain, greatly decreasing the outage probability and ergodic rate performance of the user. The closed-form expressions of ergodic rates and high signal-to-noise ratio (SNR) slopes for cell-edge users was derived in [12]. According to the results, the slope of high SNR is constant, and STAR-RIS aided NOMA systems achieve higher ergodic rates than conventional RIS aided NOMA systems. A RIS-assisted user pairing terahertz NOMA system (RTHz-NOMA) was proposed in [13]. Researches show that the proposed RTHz-NOMA system is better than the orthogonal multiple access, and the RIS can significantly enhance the sum-rate and bit error rate performance of RTHz-NOMA system.

To sum up, although relevant modeling of STAR-RIS has been carried out in the existing literature, it is still necessary to optimize the user performance of omnidirectional multi-user SEB on NOMA. Therefore, using STAR-RIS, a signal enhancement algorithm based on NOMA is proposed in this paper. This paper uses STAR-RIS to serve users on both sides. Using NOMA technology, users on both sides of STAR-RIS are formed into a user cluster, sharing the same time domain, frequency domain and code domain resources. Based on the coherence of wireless signal, a signal enhancement algorithm is designed to enhance the reflected signal and transmitted signal coherently at the users, which greatly improves the user's performance. Based on Riemannian optimization algorithm (ROA), the ergodic rates of reflection and transmission users are optimized. According to the simulation results, the proposed signal enhancement algorithm can greatly improve the ergodic rate and spectral efficiency of users.

2. System Model

The system model of proposed NOMA enhanced STAR-RIS SEB design is shown in Fig. 1, where a single antenna BS serves four single antenna users simultaneously. An array panel containing N STAR-RIS elements is deployed in the cell, which can reflect the signal to user 1 and user 2, and simultaneously transmit signal to user 3 and user 4. As the main concern is the impact of STAR-RIS on the user ergodic rate and spectral efficiency, the single-antenna narrowband model is used. It is assumed that users 1 and 2 are in the same NOMA group, whereas user 3 and user 4 are in the other NOMA group. According to the channel detection technique proposed in [14], it can be assumed that CSI is ideally known.

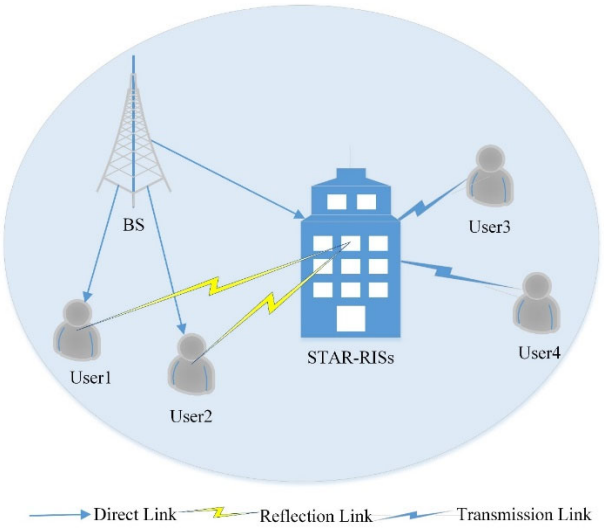

Fig. 1: STAR-RIS signal enhancement system model based on NOMA.

Without loss of generality, it is assumed that the power domain channel gains of the BS to user 1 and user 2 are $|h_1|^2$ and $|h_2|^2$. The small-scale channel vector $\mathbf{h}$ from the BS to STAR-RIS can be written as:

$$\boldsymbol{h} = \begin{bmatrix} h_{R,1} \\ \vdots \\ h_{R,N} \end{bmatrix}, \tag{1}$$

where $\mathbf{h}$ denotes the complex vector and $h_{R,n}$ represents the channel gain from the BS to the n-th STAR-RIS element.

Similarly, the reflected small-scale fading vectors $\mathbf{r}_1$ and $\mathbf{r}_2$ of STAR-RIS to user 1 and user 2 can be written as:

$$\begin{aligned} \boldsymbol{r}_1 &= [r_{1,1}, \cdots, r_{1,N}] \\ \boldsymbol{r}_2 &= [r_{2,1}, \cdots, r_{2,N}], \end{aligned} \tag{2}$$

where both $\mathbf{r}_1$ and $\mathbf{r}_2$ denote complex vectors, and $r_{1,n}$ represents the reflected channel gain of the n -th STAR-RIS element to user 1, whose fading coefficient follows the Rice distribution with fading parameter κ_1. Therefore, the reflected channel gain can be calculated as:

$$r_{1,n} = \sqrt{\frac{\kappa_1}{\kappa_1+1}} r_{1,n}^{LoS} + \sqrt{\frac{1}{\kappa_1+1}} r_{1,n}^{NLoS}, \tag{3}$$

where $r_{1,n}^{\mathrm{LoS}}$ and $r_{1,n}^{\mathrm{NLoS}}$ denote the direct and non-direct components, respectively.

The transmitted small-scale fading vectors $\mathbf{t}_3$ and $\mathbf{t}_4$ of STAR-RIS to user 3 and user 4 can be written as:

$$\begin{aligned} \boldsymbol{t}_3 &= [t_{3,1}, \cdots, t_{3,N}] \\ \boldsymbol{t}_4 &= [t_{4,1}, \cdots, t_{4,N}], \end{aligned} \tag{4}$$

where both $\mathbf{t}_3$ and $\mathbf{t}_4$ denote complex vectors, and $t_{3,n}$ represents the transmitted channel gain of the n-th STAR-RIS element to user 3, which follows the Rice distribution of fading coefficient κ_2, so the transmitted channel gain can be written as:

$$t_{3,n} = \sqrt{\frac{\kappa_2}{\kappa_2+1}} t_{3,n}^{LoS} + \sqrt{\frac{1}{\kappa_2+1}} t_{3,n}^{NLoS}, \tag{5}$$

Assume that the distance from the BS to user 1 and user 2 are d_1 and d_2, respectively, so the large scale fading of the BS to user 1 and user 2 are:

$$\begin{aligned}\varepsilon_1 &= d_1^{-\alpha 1}\\ \varepsilon_2 &= d_2^{-\alpha 1},\end{aligned} \tag{6}$$

where α_1 denotes the path loss exponent from the BS to user 1 and user 2. It is assumed that the large-scale fading of the BS to user 1 and user 2 through STAR-RIS $\varepsilon_{\mathrm{R},1}$ and $\varepsilon_{\mathrm{R},2}$ obey the scattering principle, i.e.:

$$\begin{aligned}\varepsilon_{\mathrm{R},1} &= d_{\mathrm{R}}^{-\alpha 2} d_{\mathrm{R},1}^{-\alpha 3}\\ \varepsilon_{\mathrm{R},2} &= d_{\mathrm{R}}^{-\alpha 2} d_{\mathrm{R},2}^{-\alpha 3},\end{aligned} \tag{7}$$

where d_{R}, $d_{\mathrm{R},1}$ and $d_{\mathrm{R},2}$ denote the distances from the BS to STAR-RIS, STAR-RIS to user 1 and user 2, and α_2 and α_3 represent the path fading coefficients from the BS to STAR-RIS, and from STAR-RIS to user 1 and user 2, respectively.

Similarly, large-scale fading from the BS to user 3 and user 4 through STAR-RIS can be written as:

$$\begin{aligned}\varepsilon_{\mathrm{T},3} &= d_{\mathrm{R}}^{-\alpha 2} d_{\mathrm{R},3}^{-\alpha 4}\\ \varepsilon_{\mathrm{T},4} &= d_{\mathrm{R}}^{-\alpha 2} d_{\mathrm{R},4}^{-\alpha 4},\end{aligned} \tag{8}$$

where $d_{\mathrm{R},3}$ and $d_{\mathrm{R},4}$ denote the distance from STAR-RIS to users 3 and 4, and α_4 represents the path fading coefficients from STAR-RIS to users 3 and 4.

With the aid of NOMA technology, the BS can serve four users simultaneously with SC. The equivalent transmitted signal S can be written as:

$$S = \delta_1 s_1 + \delta_2 s_2 = \delta_1 s_3 + \delta_2 s_4, \tag{9}$$

where s_1, s_2, s_3 and s_4 denote the signals of users 1, 2, 3 and 4. δ_1 and δ_2 denotes the power distribution coefficients of users 1 and 3 and users 2 and 4, respectively with $\delta_1^2 + \delta_2^2 = 1$.

In summary, the signals received by user 1 and user 2 are as follows:

$$\begin{aligned}y_1 &= \sqrt{d_1^{-\alpha 1}} h_1 pS + \sqrt{d_{\mathrm{R}}^{-\alpha 2} d_{\mathrm{R},1}^{-\alpha 3}}\,\mathbf{r}_1 \boldsymbol{\Phi}_{\mathrm{Rh}} pS + N_0\\ y_2 &= \sqrt{d_2^{-\alpha 1}} h_2 pS + \sqrt{d_{\mathrm{R}}^{-\alpha 2} d_{\mathrm{R},2}^{-\alpha 3}}\,\mathbf{r}_2 \boldsymbol{\Phi}_{\mathrm{Rh}} pS + N_0,\end{aligned} \tag{10}$$

where p denotes the transmitting power at the BS. N_0 represents the additive white Gaussian noise, which obeys a distribution with mean 0 and variance σ^2. ϕ_{R} denotes the reflection diagonal matrix of STAR-RIS, which is defined as:

$$\boldsymbol{\Phi}_{\mathrm{R}} \triangleq diag[\beta_{\mathrm{R},1}\phi_{\mathrm{R},1}, \beta_{\mathrm{R},2}\phi_{\mathrm{R},2}, \cdots, \beta_{\mathrm{R},N}\phi_{\mathrm{R},N}], \tag{11}$$

where $\beta_{\mathrm{R},n}$ and $\phi_{\mathrm{R},n}$ denote the amplitude reflection coefficient and phase reflection coefficient of the n-th STAR-RIS element, and the phase reflection coefficient satisfies $\phi_{\mathrm{R},n} = exp(j\theta_{\mathrm{R},n}), j = \sqrt{-1}, \forall n = 1,2,\cdots,N$.

Due to the distance between the BS and users 3 and 4, it is assumed that they cannot directly receive the signal from the BS. User 3 and user 4 use the transmitted signal of STAR-RIS to communicate with the BS. So they receive the signal as follows:

$$\begin{aligned}y_3 &= \sqrt{d_{\mathrm{R}}^{-\alpha 2} d_{\mathrm{R},3}^{-\alpha 4}}\,\mathbf{t}_3 \boldsymbol{\Phi}_{\mathrm{Th}} pS + N_0\\ y_4 &= \sqrt{d_{\mathrm{R}}^{-\alpha 2} d_{\mathrm{R},4}^{-\alpha 4}}\,\mathbf{t}_4 \boldsymbol{\Phi}_{\mathrm{Th}} pS + N_0,\end{aligned} \tag{12}$$

where $\boldsymbol{\Phi}_{\mathrm{T}}$ denotes the transmission diagonal matrix of STAR-RIS, which is defined as:

$$\boldsymbol{\Phi}_{\mathrm{T}} \triangleq diag\left[\beta_{\mathrm{T},1}\phi_{\mathrm{T},1}, \beta_{\mathrm{T},2}\phi_{\mathrm{T},2}, \cdots, \beta_{\mathrm{T},N}\phi_{\mathrm{T},N}\right], \tag{13}$$

where $\beta_{\mathrm{T},n}$ and $\phi_{\mathrm{T},n}$ denote the amplitude transmission coefficient and phase transmission coefficient of the n-th STAR-RIS element, respectively. The amplitude reflection coefficient and amplitude transmission coefficient meet the requirements of $\beta_{\mathrm{R},n}^2 + \beta_{\mathrm{T},n}^2 = 1, \beta_{\mathrm{R},n}^2 = \beta_{\mathrm{T},n}^2 = 0.5$ [15]. phase transmission system satisfies $\phi_{\mathrm{T},n} = exp(j\theta_{\mathrm{T},n}), \forall n = 1,2,\cdots,N$.

3. Signal enhancement algorithm

In order to enhance the signal of all users at the same time, it is assumed that the CSI is known at STAR-RIS, so the passive beamforming target of STAR-RIS can be written as:

$$\begin{aligned} &max\sqrt{d_1^{-\alpha_1}}h_1 p + \sqrt{d_{\mathrm{R}}^{-\alpha_2} d_{\mathrm{R},1}^{-\alpha_3}}\mathbf{r}_1\boldsymbol{\Phi}_{\mathrm{R}}\mathbf{h}p \\ &max\sqrt{d_2^{-\alpha_1}}h_2 p + \sqrt{d_{\mathrm{R}}^{-\alpha_2} d_{\mathrm{R},2}^{-\alpha_3}}\mathbf{r}_2\boldsymbol{\Phi}_{\mathrm{R}}\mathbf{h}p \end{aligned} \tag{14a}$$

$$\begin{aligned} &max\sqrt{d_{\mathrm{R}}^{-\alpha_2} d_{\mathrm{R},3}^{-\alpha_4}}\mathbf{t}\boldsymbol{\Phi}_{\mathrm{T}}\mathbf{h}p \\ &max\sqrt{d_{\mathrm{R}}^{-\alpha_2} d_{\mathrm{R},4}^{-\alpha_4}}\mathbf{t}\boldsymbol{\Phi}_{\mathrm{T}}\mathbf{h}p \end{aligned} \tag{14b}$$

$$S.t.\,\beta_{\mathrm{R},n} = 0.5, \beta_{\mathrm{T},n} = 0.5, \forall n = 1\cdots N \tag{14c}$$

$$\phi_{\mathrm{R},n} \in [0,2\pi), \phi_{\mathrm{T},n} \in [0,2\pi), \tag{14d}$$

where formula (14a) denotes the signal enhancement objective function of user 1 and user 2, formula (14b) brepresents the signal enhancement objective function of user 3 and user 4, formula (14c) denotes the reflection amplitude coefficients and transmission amplitude coefficients of STAR-RIS, Formula (14d) represents the reflection phase coefficients and transmission phase coefficients of STAR-RIS.

Since the wireless signal is a vector, (14a) can be rewritten as:

$$\begin{aligned} &max \parallel \sqrt{d_1^{-\alpha_1}}h_1 + \mathbf{q}_{\mathrm{R}}^H\mathbf{A}_1 \parallel^2 \\ &max \parallel \sqrt{d_2^{-\alpha_1}}h_2 + \mathbf{q}_{\mathrm{R}}^H\mathbf{A}_2 \parallel^2, \end{aligned} \tag{15}$$

where $\mathbf{A}_1 = \frac{\sqrt{2}}{2}\sqrt{d_{\mathrm{R}}^{-\alpha_2} d_{\mathrm{R},1}^{-\alpha_3}}\mathrm{diag}(\mathbf{r_1})\mathbf{h}, \mathbf{A}_2 = \frac{\sqrt{2}}{2}\sqrt{d_{\mathrm{R}}^{-\alpha_2} d_{\mathrm{R},2}^{-\alpha_3}}\mathrm{diag}(\mathbf{r_2})\mathbf{h}$. Amplitude coefficients are 1/2, and the phase function is $\mathbf{q}_{\mathrm{R}} = [\phi_{\mathrm{R},1}\cdots\phi_{\mathrm{R},N}]^H$.

In order to accomplish the goal of (15), (14) can be converted to convert again to:

$$\begin{aligned} &max \parallel \sqrt{d_1^{-\alpha_1}}h_1 + \mathbf{q}_{\mathrm{R}}^H\mathbf{A}_1 \parallel^2 + \parallel \sqrt{d_2^{-\alpha_1}}h_2 + \mathbf{q}_{\mathrm{R}}^H\mathbf{A}_2 \parallel^2 \\ &subject\ to\ \beta_{\mathrm{R},n} = \frac{1}{2}, \phi_{\mathrm{R},n} \in [0,2\pi), \forall n = 1\cdots N. \end{aligned} \tag{16}$$

To solve (16), we introduce a popular optimization based conjugate gradient algorithm, which is an efficient method to deal with non-convex optimization problems. First define that the manifold $\aleph$ is a topological space like a Euclidean space near a single point. The tangent space $T_\phi\aleph$ at a given point ϕ on the manifold $\aleph$ consists of the tangent vector ξ_ϕ of the curve γ passing through point ϕ. We define the complex circular manifold of $\phi \in \mathbb{C}$ as:

$$\aleph_{cc} = \{\phi \in \mathbb{C} | \phi^*\phi = 1\}. \tag{17}$$

The complex circular manifold $\aleph_{cc}$ is a Riemannian submanifold on $\mathbb{C}$. For $\forall x_1, x_2 \in \mathbb{C}$ in the complex plane $\mathbb{C}$ the Euclidean metric is defined as: $< x_1, x_2 >= Re\{x_1^* x_2\}$. Therefore, the tangent plane of the point $\phi \in \aleph_{cc}$ can be written as: $T_\phi \aleph_{cc} = \{z \in \mathbb{C} | < \phi, z >= 0\}$.

We then extend the one-dimensional manifold to the *N*-dimensional complex circular manifold. $\phi_{\mathrm{R},n} \in [0,2\pi), |\phi_{\mathrm{R},n}| = 1$ is the constraint condition of equation (16). Therefore, $\mathbf{q}_\mathrm{R} = [\phi_{\mathrm{R},1} \cdots \phi_{\mathrm{R},N}]^H$ forms a complex circular manifold of dimension n. The feasible region of the optimization problem (16) lies on the manifold $\aleph_{cc}$. The tangent space at point $\mathbf{q_R} \in \aleph_{cc}^N$ is given by $T_{\mathbf{q_R}} \aleph_{cc}^N = \{\mathbf{z} \in \mathbb{C}^N | Re\{\mathbf{z} \circ \mathbf{q}_\mathbf{R}^*\} = \mathbf{0}_N\}$.

Let the objective function of the optimization problem (16) be:$f(\mathbf{q}_\mathrm{R}) = \| \sqrt{d_1^{-\alpha_1}} h_1 + \mathbf{q}_\mathrm{R}^H \mathbf{A}_1 \|^2 + \| \sqrt{d_2^{-\alpha_1}} h_2 + \mathbf{q}_\mathrm{R}^H \mathbf{A}_2 \|^2$, which gradient function is:

$$\nabla f(\mathbf{q}_\mathrm{R}) = 2(\mathbf{A_1 A_1}^H \mathbf{q}_\mathrm{R} + \mathbf{A_1}(\sqrt{d_1^{-\alpha_1}})^* h_1) + 2(\mathbf{A_2 A_2}^H \mathbf{q}_\mathrm{R} + \mathbf{A_2}(\sqrt{d_2^{-\alpha_1}})^* h_2) \quad (18)$$

Similar to Euclidean space, there is a tangent vector direction in which the objective function grows fastest, which is called Riemann gradient. Since the complex circular manifold $\aleph_{cc}^N$ is a Riemannian submanifold on *N*-dimensional complex space $\mathbb{C}^N$, the Riemannian gradient of function $f(\mathbf{q}_\mathrm{R})$ at point $\mathbf{q}_\mathrm{R}$ (represented by $\mathbf{grad} f_\mathrm{R}$) is the orthogonal projection of the Euclidean gradient ∇f_R. Therefore, the Riemannian gradient at the point $\mathbf{q}_\mathrm{R}$ on the complex circular manifold $\aleph_{cc}^N$ can be written as:

$$\mathbf{grad} f_\mathrm{R} = \nabla f_\mathrm{R}(\mathbf{q}_\mathrm{R}) - \mathbf{Re}\{\nabla f_R(\mathbf{q}_\mathrm{R})^\circ \mathbf{q}_\mathrm{R}^*\}^\circ \mathbf{q}_\mathrm{R}, \quad (19)$$

where $\mathbf{grad}$ is the gradient symbol.

Then, we can determine that the search direction of the conjugate gradient method is:

$$d = -\mathbf{grad} f_\mathrm{R} + \tau \Omega_r(d), \quad (20)$$

where$\Omega_r(d) = d - \mathbf{Re}\{d^\circ \mathbf{q}_\mathrm{R}^*\}\mathbf{q}_\mathrm{R}$.

However, d_k and d_{k+1} in manifold optimization lie in two different tangent spaces. Instead of directly performing operations involving different tangent spaces, we give a mapping from the tangent space to the manifold itself, i.e. :

$$(\mathbf{q}_\mathrm{R})_i \leftarrow \frac{(\mathbf{q}_\mathrm{R} + \alpha d)_i}{|(\mathbf{q}_\mathrm{R} + \alpha d)_i|} \quad (21)$$

where α is the search step size.

According to the steps of Formula (19) to formula (21), the passive beam forming algorithm is shown in **Algorithm 1**. According to theorem 4.3.1 in [16], it is ensured that **Algorithm 1** converges to the critical point, that is, the gradient of the objective function at this point is zero. The RIS amplitude and phase of the reflection part can be solved by using Riemannian manifold optimization. Similarly, the transmission part is also apply Riemannian manifold optimization solution.

Algorithm 1 Passive Beamforming Conjugate gradient algorithm based on Manifold Optimization

Input: $\sqrt{d_1^{-\alpha_1}}, \sqrt{d_2^{-\alpha_1}}, h_1, h_2, \mathbf{A_1}, \mathbf{A_2}$

Output: $\mathbf{q}_{\mathrm{R}}$

1: Randomly initialize the reflection phase matrix of RIS $\mathbf{q}_{\mathrm{R0}} \in \aleph_{cc}^{N}$, calculate $d_0 = -\mathbf{grad} f_{\mathrm{R0}}$, display k =0

2: repeat

3: Select linear search step α_k

4: Find $\mathbf{q}_{\mathrm{R1}}$ by formula (21)

$$\mathbf{q}_{\mathrm{R}(k+1)} = \frac{(\mathbf{q}_{\mathrm{R}k} + \alpha_k d)_n}{|(\mathbf{q}_{\mathrm{R}k} + \alpha_k d)_n|}$$

5: According to formulas (18) and (19), caculate $g_{k+1} = \mathbf{grad} f_{\mathrm{R}(k+1)}$

6: According to the formula (20), the transpose vector g_k of the gradient $\overline{g}_k$ and the conjugate direction d_k of $\overline{d}_k$ are calculated:

$$\overline{g}_k = g_k - Re\{g_k \circ q^*_{\mathrm{R}(k+1)}\} \circ q_{\mathrm{R}(k+1)}$$

$$\overline{d}_k = d_k - Re\{d_k \circ q^*_{R(k+1)}\} \circ q_{R(k+1)}$$

7: calculate $\tau_k = \frac{g_{k+1}^H g_{k+1}}{\overline{g}_k^H \overline{g}_k}$

8: Calculate conjugate direction $d_{k+1} = -g_{k+1} + \tau_k \overline{d}_k$

9: Update $k \leftarrow k+1$

10: Until it converges

11: return $\mathbf{q}_{\mathrm{R}} = \mathbf{q}_{\mathrm{R}(k+1)}$

Therefore, based on the passive beamforming design of equations passive (15) to (19), the received signal amplitude of user 1 can be rewritten as:

$$y_1 = \sqrt{d_1^{-\alpha_1}} |h_1| pS + |\mathbf{q}_{\mathrm{R}}^H \mathbf{A}_1| pS + N_0. \tag{22}$$

Based on NOMA protocol, the channel gain of user 1 is strong, so user 1 can use SIC technology to detect and delete the Signal of user 2, and its signal-to-interference-plus-noise-ratio (SINR) can be written as:

$$SINR_{1\to 2} = \frac{p|\overline{h_1}|^2 \delta_2^2}{\sigma^2 + p|\overline{h_1}|^2 \delta_1^2}, \tag{23}$$

where $|h_1|^2 = (\sqrt{d_1^{-\alpha_1}} |h_1| + |\mathbf{q}_{\mathrm{R}}^H \mathbf{A}_1|)^2$.

After user 1 successfully detects the signal of user 2, user 1 can delete the signal of user 2 and detect the signal of user 1, and its SNR can be written as:

$$SNR_1 = \frac{|\overline{h_1}|^2 \delta_1^2 p}{\sigma^2}, \tag{24}$$

where $|h_2|^2 = (\sqrt{d_2^{-\alpha_1}} |h_2| + |\mathbf{q}_{\mathrm{R}}^H \mathbf{A}_2|)^2$.

Based on the NOMA protocol, the channel gain of user 2 is weak, so user 2 regards the signal of user 1 as interference, and its SINR can be written as:

$$SINR_2 = \frac{|\overline{h_2}|^2 \delta_2^2 p}{|\overline{h_2}|^2 \delta_1^2 p + \sigma^2}. \tag{25}$$

Similar to the process of (15) to (25), the transmit passive beamforming design can be completed.

The ergodic rates $\overline{\mathrm{R}_1}$ and $\overline{\mathrm{R}_2}$ for user 1 and user 2 can be defined as:

$$\begin{aligned} \overline{\mathrm{R}_1} &= \mathrm{E}(\log_2(1 + SNR_1)) \\ \overline{\mathrm{R}_2} &= \mathrm{E}(\log_2(1 + SINR_2)), \end{aligned} \tag{26}$$

where $\mathrm{E}()$ denotes the expectation function.

The ergodic rates $\overline{\mathrm{R}_3}$ and $\overline{\mathrm{R}_4}$ for user 3 and user 4 can be defined as:

$$\begin{aligned} \overline{\mathrm{R}_3} &= \mathrm{E}(\log_2(1 + SNR_3)) \\ \overline{\mathrm{R}_4} &= \mathrm{E}(\log_2(1 + SINR_4)). \end{aligned} \tag{27}$$

Performance Evaluation

In this section, the proposed signal enhancement algorithm is verified by simulation. Monte Carlo method is used to compare the ergodic rates of user 1 and 2 and user 3 and 4, so as to show the performance gain of the proposed STAR-RIS signal enhancement algorithm. The Monte Carlo simulation is repeated 10^7 times. The bandwidth is set to BW = 1MHz, and the power of the additive white Gaussian noise is $\sigma^2 = -174 + 10log_{10}(BW)dBm$. Based on NOMA protocol, the power distribution coefficient can be set to $\delta_1^2 = 0.4$ and $\delta_2^2 = 0.6$. Other simulation parameters are shown in Table 1.

Table 1: Simulation Parameter

The distance from BS to user 1 and 2	60m
The distance from BS to STAR-RIS	80m
The distance from STAR-RIS to user 1 and 2	30m
The distance from STAR-RIS to user 3 and 4	35m
Path loss exponent from BS to user 1 and 2	3
Path loss exponent from BS to STAR-RIS	2.6
Path loss exponent from STAR-RIS to user 1 and 2	2.8
Path loss exponent from STAR-RIS to user 3 and 4	2.6
The amplitude transmission coefficient of STAR-RIS	0.5
The amplitude reflection coefficient of STAR-RIS	0.5
The power distribution coefficient of user 1 and 3	0.4
The power distribution coefficient of user 2 and 4	0.6

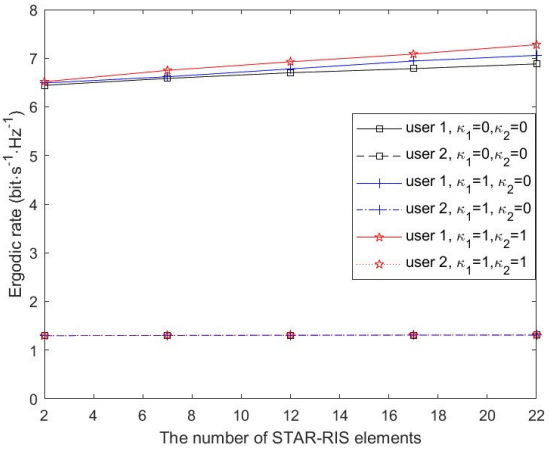

Fig. 2: The ergodic rate versus different number of STAR-RIS element and channel fading coefficient of reflection users.

To compare the effects of the channel fading coefficient and the number of STAR-RIS elements on the user 1 and user 2 ergodic rates, we set the channel fading coefficient to $\kappa_1, \kappa_2 = 0,1$, and the ergodic rate performance of user 1 and user 2 is shown in Fig. 2. By comparing the red curve, blue curve and black curve, it can be seen that when the fading coefficient of the channel from the BS to STAR-RIS or STAR-RIS to user 1 increases, the ergodic rate of user 1 increases. The same conclusion can be drawn by comparing the red dotted line, blue dotted line and black dotted line in the figure, when the channel decay coefficient from BS to STAR-RIS or STAR-RIS to user 2 increases, the ergodic rate of user 2 increases.

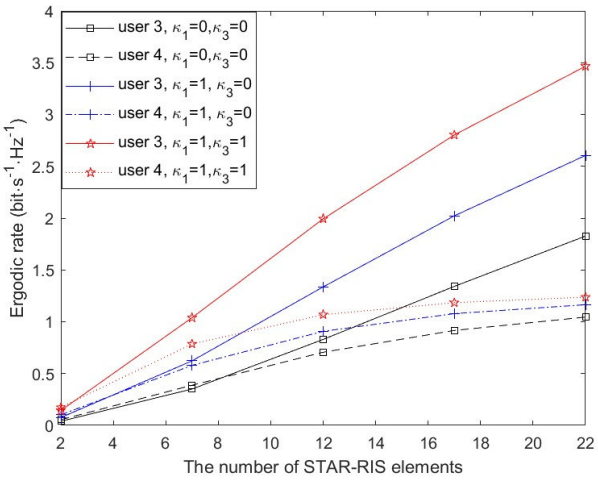

Fig. 3: The ergodic rate versus different number of STAR-RIS element and channel fading coefficient of transmission users.

To compare the effects of the channel fading coefficient and the number of STAR-RIS elements on the user 3 and user 4 ergodic rates, we set the channel fading coefficient to $\kappa_1, \kappa_3 = 0,1$, and the ergodic rate performance of user 3 and user 4 is shown in Fig. 3. By comparing the red curve, blue curve and black curve, it can be seen that when the fading coefficient of the channel from the BS to STAR-RIS or STAR-RIS to user 3 increases, the ergodic rate of user 3 increases. The same conclusion can be drawn by comparing the red dotted line, blue dotted line and black dotted line in the figure, when the channel decay coefficient from BS to STAR-RIS or STAR-RIS to user 4 increases, the ergodic rate of user 4 increases. It also proves that the channel parameters have a great influence on the proposed NOMA signal enhancement algorithm based on STAR-RIS. In addition, it can be seen that when the number of STAR-RIS increases, the ergodic rates of user 3 increase, and the high SNR slope of user 3 increases, which indicates that increasing the number of STAR-RIS has a great impact

on the ergodic rate of user 3. This is because in NOMA, user 3 is not affected by interference, while user 4 is affected by homologous interference.

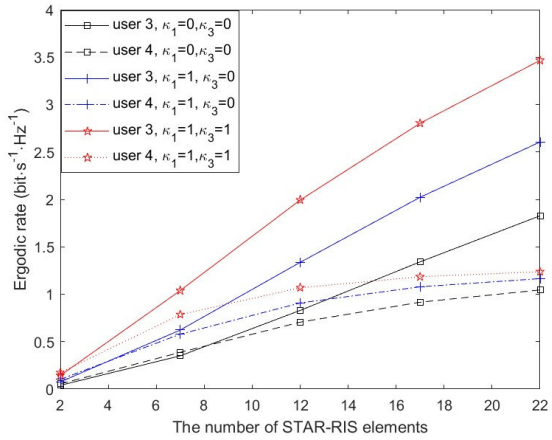

Fig. 4: The influence of different algorithms on the energy efficiency of users.

Fig. 4 illustrates the energy efficiency of users across various algorithms. It reveals that employing phase randomization with STAR-RIS leads to an energy efficiency enhancement of approximately 0.29 bit/s/J compared to scenarios without the STAR-RIS algorithm. Furthermore, upon implementing the ROA, an additional energy efficiency boost of about 0.16 bit/s/J is achieved, underscoring the algorithm's remarkable efficacy. Moreover, when STAR-RIS directs all energy to user 3 and user 4, their energy efficiency diminishes. This observation suggests a prioritization of closer-to-base-station users in the proposed model, aimed at enhancing the system's energy efficiency.

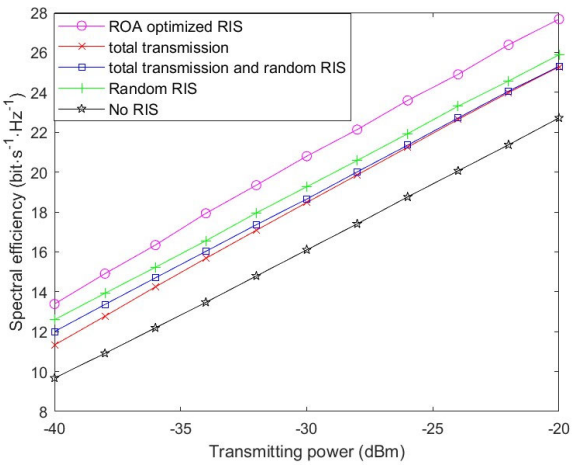

Fig. 5: The influence of different algorithms on the spectral efficiency of users.

Fig. 5 compares the spectral efficiency of users with different algorithms. It can be seen that the phase randomization of STAR-RIS can improve the spectral efficiency of about 3.6bit/s/Hz compared with the absence of STAR-RIS. After using the proposed ROA, the spectral efficiency can be increased by about 1.8bit/s/Hz, which verifies the superiority of the proposed algorithm. In addition, it can be seen that when STAR-RIS transmits all the energy to user 3 and user 4, the spectral efficiency is low. This phenomenon also indirectly indicates that the proposed model will give priority to the users who are closer to the BS to improve the spectral efficiency of the system.

4. Conclusions

In this paper, a STAR-RIS signal enhancement algorithm based on NOMA is proposed, which benefits from the omnidirectional property of STAR-RIS and can serve users on both sides of STAR-RIS simultaneously and at the same frequency. By using ROA, the coherent superposition of the

user's signal can greatly improve the user's SNR and improve the ergodic rate performance. The proposed STAR-RIS signal enhancement algorithm based on NOMA is applied to the single antenna scene. The next step will discuss the joint design of the active beamforming of the BS, the passive beamforming of the STAR-RIS and the detection vector of the user in the multi-antenna field. In addition, in order to be more suitable for the actual application scenario, the number of users and user mobility also have important research value, and will be in the future.

Acknowledgement

This work was supported in part by the Fundamental Research Funds for the Central Universities under Grant 2023JBZY012, in part by the National Natural Science Foundation for Young Scientists of China under Grant 62201028, in part by Young Elite Scientists Sponsorship Program by CAST under Grant 2022QNRC001, in part by the Beijing Natural Science Foundation L232041, and in part by the Marie Skłodowska-Curie Fellowship under Grant 101106428. The corresponding author of this paper is Tianwei Hou.

References

[1] S. Yrjölä, M. Matinmikko-Blue, and P. Ahokangas, "Developing 6G Visions with Stakeholder Analysis of 6G Ecosystem," in 2023 Joint European Conference on Networks and Communications & 6G Summit (EuCNC/6G Summit), 2023, pp. 705-710.

[2] L. Yang, P. Li, Y. Yang, S. Li, I. Trigui, and R. Ma, "Performance Analysis of RIS-Aided Networks With Co-Channel Interference," IEEE Communications Letters, vol. 26, no. 1, pp. 49-53, 2022.

[3] Z. Zhakipov, K. M. Rabie, X. Li, and G. Nauryzbayev, "Accurate Approximation to Channel Distributions of Cascaded RIS-Aided Systems With Phase Errors Over Nakagami-m Channels," IEEE Wireless Communications Letters, vol. 12, no. 5, pp. 922-926, 2023.

[4] M. Li, S. Zhang, Y. Ge, Z. Li, F. Gao, and P. Fan, "STAR-RIS Aided Integrated Sensing and Communication over High Mobility Scenario," IEEE Transactions on Communications, pp. 1-1, 2024.

[5] H. Chang, X. Kang, H. Lei, T. A. Tsiftsis, G. Pan, and H. Liu, "STAR-RIS-Aided Covert Communications in MISO-RSMA Systems," IEEE Transactions on Green Communications and Networking, pp. 1-1, 2024.

[6] G. Sun, R. He, Z. Ma, B. Ai, and Z. Zhong, "A 3D Geometry-Based Non-Stationary MIMO Channel Model for RIS-Assisted Communications," in 2021 IEEE 94th Vehicular Technology Conference (VTC2021-Fall), 2021, pp. 1-5.

[7] Y. Pan, Z. Qin, J. B. Wang, Y. Chen, H. Yu, and A. Tang, "Joint Deployment and Beamforming Design for STAR-RIS Aided Communication," IEEE Communications Letters, vol. 27, no. 11, pp. 3083-3087, 2023.

[8] A. Hesam and A. H. Bastami, "NOMA-Based Transmission in Half-Duplex Two-Way Relay Network," in 2020 28th Iranian Conference on Electrical Engineering (ICEE), 2020, pp. 1-6.

[9] P. Sharma, A. Kumar, and M. Bansal, "Performance Analysis of Downlink NOMA System with Diversity Combining Schemes over k-μ Fading Channel," in 2022 IEEE 6th Conference on Information and Communication Technology (CICT), 2022, pp. 1-5.

[10] M. A. Arfaoui, A. Ghrayeb, C. Assi, and M. Qaraqe, "CoMP-Assisted NOMA and Cooperative NOMA in Indoor VLC Cellular Systems," IEEE Transactions on Communications, vol. 70, no. 9, pp. 6020-6034, 2022.

[11] T. Hou, Y. Liu, Z. Song, X. Sun, Y. Chen, and L. Hanzo, "Reconfigurable Intelligent Surface Aided NOMA Networks," IEEE Journal on Selected Areas in Communications, vol. 38, no. 11, pp. 2575-2588, 2020.

[12] B. Zhao, C. Zhang, W. Yi, and Y. Liu, "Ergodic Rate Analysis of STAR-RIS Aided NOMA Systems," IEEE Communications Letters, vol. 26, no. 10, pp. 2297-2301, 2022.

[13] M. H. Kumar, S. Sharma, K. Deka, and M. K. Sharma, "RIS-assisted User Pairing NOMA System for THz Communications," in 2023 National Conference on Communications (NCC), 2023, pp. 1-6.

[14] J. Zhang, C. Qi, P. Li, and P. Lu, "Channel Estimation for Reconfigurable Intelligent Surface Aided Massive MIMO System," in 2020 IEEE 21st International Workshop on Signal Processing Advances in Wireless Communications (SPAWC), 2020, pp. 1-5.

[15] Z. Li, M. Hua, Q. Wang, and Q. Song, "Weighted Sum-Rate Maximization for Multi-IRS Aided Cooperative Transmission," IEEE Wireless Communications Letters, vol. 9, no. 10, pp. 1620-1624, 2020.

[16] T. Bai and R. W. Heath, "Coverage and Rate Analysis for Millimeter-Wave Cellular Networks," IEEE Transactions on Wireless Communications, vol. 14, no. 2, pp. 1100-1114, 2015.